THE ASTROPHYSICAL JOURNAL, 510:892–904, 1999 January 10

MAGNETIC ACCRETION AND PHOTOPOLARIMETRIC VARIABILITY IN CLASSICAL T TAURI STARS

KEIVAN STASSUN[1] AND KENNETH WOOD[2]
Received 1998 March 23; accepted 1998 August 18

ABSTRACT

We employ a Monte Carlo radiation transfer code to investigate the multiwavelength photopolarimetric variability arising from a spotted T Tauri star surrounded by a dusty circumstellar disk. Our aim is to assess the ability of the magnetic accretion model to explain the observed photopolarimetric variability of classical T Tauri stars and to identify potentially useful observational diagnostics of T Tauri star/disk/spot parameters. We model a range of spot sizes, spot latitudes, inner disk truncation radii, and system inclination angles, as well as multiple disk and spot geometries. We find that the amplitude, morphology, and wavelength-dependence of the photopolarimetric variability predicted by our models are generally consistent with existing observations; a flared disk geometry is required to reproduce the largest observed polarization levels and variations. Our models can further explain stochastic polarimetric variability if unsteady accretion is invoked, in which case irregular (but correlated) photometric variability is predicted, in agreement with observations. We find that variability in percent polarization is by itself an unreliable diagnostic, because certain system geometries do not produce any variability in linear polarization (contrary to the commonly held notion that hot spots will necessarily produce periodic polarimetric variability). Observations of variability in polarization position angle, however, could provide useful constraints on system inclination. The observation of wavelength-dependent polarization position angles, attributed by some to interstellar effects, is naturally explained by our models. Certain system geometries yield peculiar photometric light curve morphologies, the observation of which could also serve to constrain system inclination. We do not find useful diagnostics of disk truncation radius, nor do we find significant differences when we model the spots as rings. We also investigate the reliability of modeling spot parameters via analytic fits to multiband photometric variations. We find that commonly used analytic models consistently recover input model parameters but that inferred spot temperatures are more sensitive to uncertainties in the photometric data than previous modeling would suggest.

Subject headings: accretion, accretion disks — polarization — radiative transfer — stars: pre–main-sequence — stars: rotation — stars: spots

1. INTRODUCTION

T Tauri stars are low-mass pre–main-sequence (PMS) stars with a rich history of observational and theoretical study, dating back to Joy's (1945) discovery paper. Seen initially as stellar oddities, T Tauri stars have become paradigmatic of early stellar evolution. The data paint an intricate picture of stars in their earliest evolutionary stages: Excess infrared and submillimeter emission indicate extended circumstellar disks of gas and dust; excess ultraviolet emission, hydrogen emission lines, and erratic brightness variations suggest hot accretion zones, where infalling material impacts the stellar surface; photospheric spots, similar in nature to sunspots, reveal magnetic activity.

Despite this wealth of information regarding the nature of T Tauri stars, they remain somewhat enigmatic objects. In particular, our understanding of the accretion process is at present incomplete and is currently a subject of intense study. Until recently, the commonly accepted mechanism for accretion of circumstellar material onto stellar surfaces was via a "boundary layer" model (e.g., Basri & Bertout 1989), in which disk material falls onto the star along the midplane, producing an equatorial ring of hot ($\sim$10,000 K), optically thin material. More recently, however, attention has turned to an accretion model that attempts to account for the influence of the stellar magnetic field and that serves to explain such phenomena as the observed bimodal rotation period distribution (e.g., Attridge & Herbst 1992), inverse P Cygni line profiles (Hartmann, Hewett, & Calvet 1994; Edwards et al. 1994), and the presence of photospheric hot spots (Bouvier et al. 1993; Herbst et al. 1994).

The magnetic accretion model (Ghosh & Lamb 1979a, 1979b; Königl 1991; Shu et al. 1994; Ostriker & Shu 1995; Najita 1995) as applied to PMS stars is characterized by the following: a star surrounded by a geometrically thin, optically thick, circumstellar disk truncated within a certain inner radius; a stellar dipole magnetic field that threads the disk; and accretion "streams" of disk material that flow along field lines and impact the star at the magnetic poles, producing hot spots there (or "rings;" Mahdavi & Kenyon 1998). The presence of hot spots or rings on the stellar surface has observable consequences. Periodic photometric variations will be produced as the star's rotation brings the spots into and out of view; periodic polarimetric variations have also been predicted (e.g., Gullbring & Gahm 1996) because of periodically varying illumination of the disk by the spots.

Photometric variability is a ubiquitous characteristic of T Tauri stars. And *periodic* photometric variability has now been confirmed in hundreds of systems in star-forming regions throughout the Galaxy: Bouvier et al. (1993) in their study of 24 T Tauri stars in Taurus-Auriga found evidence for periodic variability in at least 20; in Lupus Wichmann et al. (1998) found periodic variability in 34 of 46 targets

[1] Astronomy Department, University of Wisconsin, 475 North Charter Street, Madison, WI 53706; keivan@astro.wisc.edu.
[2] Smithsonian Astrophysical Observatory, 60 Garden Street, Cambridge, MA 02138; kenny@claymore.harvard.edu.

studied; in Orion Herbst and collaborators have, to date, identified 75 periodic variables (Choi & Herbst 1996); and in NGC 2264 Makidon et al. (1997) find some 200 periodic variables. The periods of the observed variability range from about 1 day to several tens of days, with the short period limit likely determined by the sampling of the observing programs. In most systems the spots persist stably over multiple rotation periods and, in some cases, over multiple observing seasons. A favored explanation for such periodic variability is stellar spots; periodic photometric variations have been modeled analytically in numerous systems by several authors (e.g., Bouvier et al. 1993) within this context in order to derive spot properties (size, temperature, and position). Taken at face value, the results of such modeling suggest that spots on weak-lined T Tauri systems tend to be cool (cooler than the photosphere), while classical T Tauri systems can possess both hot and cool spots. In some systems, hot and cool spots have been found concurrently (e.g., Vrba et al. 1986). Although hot accretion spots seem to manifest themselves most often as irregular variables, stable photometric variability due to hot spots has been seen in numerous systems (e.g., Bouvier et al. 1993). It is these systems that we model in this study.

Polarimetric variability has also been detected in numerous systems (e.g., Drissen, Bastien, & St. Louis 1989), although so far *periodic* polarimetric variability has not been found[3]. As a result, alternative mechanisms for the observed variability—such as obscuration by circumstellar material—have been proposed (e.g., Gullbring & Gahm 1996). More typically, erratic polarimetric variability of $\sim 0.5\%$ has been observed, with only a few systems exhibiting variability of 2%–3% (Gullbring & Gahm 1996). Numerous systems have exhibited large position angle variations as well. In a few cases, photometric and polarimetric variability have been observed to be anticorrelated (Drissen et al. 1989; Gullbring & Gahm 1996) in the sense of lower polarization at maximum light.

Detailed calculations of spot/ring geometries have been carried out (Mahdavi & Kenyon 1998) as well as Monte Carlo simulations of photopolarimetric variability of a spotted star plus a flat disk (Wood et al. 1996), where predictions were made of the V-band photopolarimetric variability for one particular star-spot-disk geometry. In this paper, we extend the work of Wood et al. and perform simulations of the photopolarimetric variability at several wavelengths (U, V, I, and K) and for a large grid of spot latitude, spot size, and system inclination geometries. We also investigate the effects of a flared disk and of ringlike spots on the resulting photopolarimetric variability. As the magnetic accretion paradigm gains popularity as a generalized model for accretion in T Tauri stars, it is timely to confront the model with the existing data and to seek out robust observational diagnostics of accretion signatures in these systems. Thus our aim here is to assess the ability of the magnetic accretion model to explain existing observations of photopolarimetric variability in classical T Tauri stars, to identify observational diagnostics that may prove useful in constraining T Tauri system spot/disk properties of interest, and to make predictions of unusual or otherwise distinctive observable phenomena arising from the magnetic accretion model. Basic physical properties of spots such as temperature and size are particularly germane to this discussion, and so we examine the validity of an analytic inversion technique commonly used to infer spot properties from photometric variability by inverting our simulated data to retrieve known spot temperatures and sizes.

In § 2 we describe the Monte Carlo radiation transfer technique employed. The results of our simulations are presented in § 3, wherein we discuss potentially useful photopolarimetric diagnostics of T Tauri system parameters. We compare our models to observations in § 4 and generally discuss the ability of the magnetic accretion model to explain the existing photopolarimetric data. In § 5 we examine an analytic inversion technique commonly used to model observations of photometric variability. Lastly, we summarize our findings in § 6.

2. MODEL PARAMETERS AND RADIATION TRANSFER TECHNIQUE

The models that we investigate comprise a central spherical star of temperature T_*, with two diametrically opposed circular spots with radii θ_s, located at latitudes $\pm\phi_s$, both with temperature T_s. This spotted star is surrounded by a dusty equatorial circumstellar disk with inner and outer radii $R_{\rm in}$ and $R_{\rm max}$. We investigate both flat- and flared-disk geometries. The radiation transfer is performed with the Monte Carlo technique.

2.1. *Stellar Parameters*

For all our simulations we keep the stellar and spot temperatures fixed at $T_* = 4000$ K and $T_s = 10{,}000$ K. These parameters are consistent with those typically quoted for classical T Tauri stars; T Tauri stars are typically of spectral type early K and later, and detailed spectroscopic studies of classical T Tauri stars typically reveal featureless, hot "veiling" components that are bluer than photospheric colors (e.g., Basri & Batalha 1990). The parameters that we vary are the spots' angular size on the star, θ_s, and the latitude of the diametrically opposed spots, $\pm\phi_s$. We investigate spots with covering factors of 6%, 2%, and 0.07% of a hemisphere ($\theta_s = 20°$, $11\overset{\circ}{.}5$, and $6\overset{\circ}{.}6$, respectively) and choose spot latitudes in the range $45° < \phi_s < 80°$, thus simulating low- and high-latitude spots.

Strictly speaking, theory predicts that the geometry of accretion streams result in hot accretion "rings" on stellar surfaces (Mahdavi & Kenyon 1998; Kenyon et al. 1994) as opposed to the simple "spot" accretion geometry we have modeled. Our Monte Carlo technique is capable of modeling these more complex geometries if desired, but we find that modeling the accretion geometry as rings as opposed to spots does not have an observable effect on the photopolarimetry arising from T Tauri systems (§ 3.3). Thus, for the sake of simplicity and for computational ease, we model the accretion geometry as simple spots with parameters ϕ_s and θ_s.

2.2. *Disk Geometry*

We consider two geometries for the circumstellar disk. The first is the flat disk used by Wood et al. (1996). The geometry is given by

$$\rho = \frac{\rho_0}{x^2 + y^2 + z^2/b^2} \,. \tag{1}$$

[3] Periodic polarimetric variability has been reported for RY Lup (see references in Drissen et al. 1989), but we have been unsuccessful in tracing original publication of this result.

This particular form for the circumstellar geometry enables the Monte Carlo radiation transfer to proceed rapidly, since the randomly chosen scattering and absorbing locations are found analytically and numerical integration is not required. We choose $b = 10^{-3}$, which yields a very flat, disklike structure, and set the equatorial optical depth $\tau_{eq} = 10^3$. We have kept the equatorial optical depth fixed for all wavelengths and only change the dust scattering parameters with wavelength (see § 2.3). For the more realistic case of a flared disk geometry, we set the disk optical depth according to the wavelength-dependent opacity.

The second geometry we consider is a flared disk, as prescribed by Shakura & Sunyaev (1973),

$$\rho = \rho_0 \exp\{-\tfrac{1}{2}[z/h(\varpi)]^2\}/\varpi^{\alpha}, \quad (2)$$

where ϖ is the radial coordinate in the disk midplane. The scale height increases with radius according to

$$h = h_0\left(\frac{\varpi}{R_*}\right)^{\beta}. \quad (3)$$

The degree of flaring, β, lies in the range $9/8 < \beta < 5/4$ (Kenyon & Hartmann 1987), and the scale height at the stellar surface is typically taken to be $h_0 = 0.03R_*$. For our simulations we adopt $\alpha = 15/8$, $\beta = 9/8$, $h_0 = 0.025R_*$, and a disk mass of $M_{disk} = 1 \times 10^{-3}\ M_\odot$. For both flat and flared disks, we set the outer disk radius to be $R_{max} = 100$ AU, and we vary the disk truncation radius, R_{in} from R_* (no hole) to $15R_*$, thus covering the range of values generally quoted for inner disk holes (e.g., Beckwith et al. 1990; Kenyon, Yi, & Hartmann 1996).

2.3. *Dust Opacity and Scattering Parameters*

The circumstellar dust is assumed to have the same properties as a Mathis, Rumpl, & Nordsieck (1977) interstellar dust mixture with a total opacity, κ, and albedo, a. The scattering phase function is modeled by a Heyney-Greenstein phase function with asymmetry parameter, g, and polarization, p. The variation of the dust parameters with wavelength is presented in Table 1. It is possible that the circumstellar dust properties we adopt are different from interstellar dust. However, Whitney, Kenyon, & Gómez (1997) found that these parameters provide a good match to the colors of Taurus protostars, and we adopt them for our simulations also (although our Monte Carlo code could use any dust mixture just as easily).

2.4. *Radiation Transfer*

The Monte Carlo radiation transfer technique has been used in previous investigations of dust scattering and absorption in the circumstellar environments of T Tauri stars (e.g., Whitney & Hartmann 1992, 1993; Whitney et al. 1997; Fischer, Henning, & Yorke 1994; Bastien & Menard 1988). Our code simulates the transfer of "photon packets" through the circumstellar disk, with the output for the present investigation being the spatially unresolved flux and polarization. Since the disk is illuminated by an asymmetric source (spotted star), when the photons exit the system we place them into direction-of-flight bins that are determined from the photon's latitudinal and azimuthal directions (Wood et al. 1996). The stellar photons are released from the star and spots in proportion to the relative luminosities and surface areas of the star and spots. We assume that the luminosities of the star and spots are Planck functions, B_λ. Therefore, the relative number of photons released from the spot and star at a given wavelength is

$$\frac{N_s}{N_*} = \frac{(1 - \cos\theta_s)}{(\cos\theta_s)}\frac{B_\lambda(T_s)}{B_\lambda(T_*)}, \quad (4)$$

where again θ_s is the spot angular radius. The different wavelengths that we investigate are therefore simulated by releasing spot and stellar photons according to this equation, and the opacity and scattering parameters are those presented in Table 1. In our simulations we assume that all the photons originate from the star and neglect any disk emission. This is a reasonable assumption at optical wavelengths. However, for systems in which the disk extends to the stellar surface, we would expect there to be significant disk emission in the K band due to reprocessing of stellar radiation and/or accretion luminosity (Adams, Lada, & Shu 1987; Kenyon & Hartmann 1987). In the simulations where $R_{in} = R_*$, our K light curves are likely to be in error. For the simulations with larger R_{in}, the star dominates the flux at K, and it is valid that we ignore disk emission.

3. RESULTS OF MODELS

We have investigated 27 different system geometries that arise from our choices of three spot sizes, three spot latitudes, and three values for the inner disk truncation radius. For each geometry we have light curves at 10 inclination angles in each of the U, V, I, and K passbands (the fluxes computed are actually the monochromatic fluxes at the central wavelength of the passband). For the flat disk simulation we therefore have 1080 simulated light curves. We have also investigated flared disks for a subset of the system geometries in order to ascertain the effects of a more realistic disk geometry on the light curves. A summary of the relevant model parameters, with the ranges of values over which we vary them, is given in Table 2.

We begin this section by describing the predominant effects on the photopolarimetry arising from changes in the

TABLE 1

DUST PARAMETERS

Passband	κ	a	g	p
U	360	0.54	0.48	0.26
V	219	0.54	0.44	0.43
I	105	0.49	0.29	0.70
K	20	0.21	0.02	0.93

NOTE—Based on the Mathis et al. (1977) grain size distribution with optical constants from Draine (1985) and Draine & Lee (1984, 1987). Polarization values are from White (1979).

TABLE 2

MODEL PARAMETERS

Parameter	Values
T_* (K)	4000
T_s (K).....	10000
λ	U, V, I, K
ϕ_s (deg).....	$\pm$45, 65, 80
θ_s (deg)	6.6, 11.5, 20
i (deg)	18, 32, 41, 50, 57, 63, 70, 76, 81, 87
R_{in}	R_*, $3R_*$, $15R_*$

system parameters with the flat disk geometry. We then investigate the flared disk geometry and report the differences on the light curves for the flat and flared disks. As might be expected, there is considerable degeneracy among the parameters in our models; a given set of model parameters is not generally prescriptive in a quantitative way of any single photopolarimetric diagnostic we have studied. Thus, we attempt in this section to describe those features of photopolarimetric variability which, if observed, would be most useful, either individually or in combination, in constraining T Tauri system parameters. We end this section by briefly exploring the effect on observables of using a ringlike spot geometry (as in Mahdavi & Kenyon 1998).

3.1. *Flat Disks*

We have employed a simplistic disk geometry for the bulk of our modeling for computational expedience. The simple density structure of the disk (eq. [1]) has the advantage that the optical depth calculation in the radiation transfer is computed analytically. Unfortunately, this simple density structure and in particular our use of a wavelength-independent midplane optical depth does possess some undesirable properties. In particular, a number of our models show light from the spot on the lower hemisphere "leaking" through the optically thin outer disk regions in nearly edge-on viewing geometries. In edge-on cases, therefore, the flared disk geometry we consider in § 3.2 is more realistic.

We now detail the effect on the light curves of varying the spot size, latitude, truncation radius, inclination, and wavelength. In Figures 1–3 we present a graphical summary of the predominant effects on photometric and polarimetric variability as a result of changing the following key system parameters: (1) spot latitude (ϕ_s), (2) inner disk truncation radius ($R_{\rm in}$), and (3) inclination (i).

3.1.1. *Spot Size and Latitude*

For a given spot latitude and system inclination, we find that changing the spot size has only a minor effect on the magnitude of the photometric variations (variability increases slightly as θ_s increases). Our analysis of analytic inversion techniques (§ 5) confirms that amplitudes of

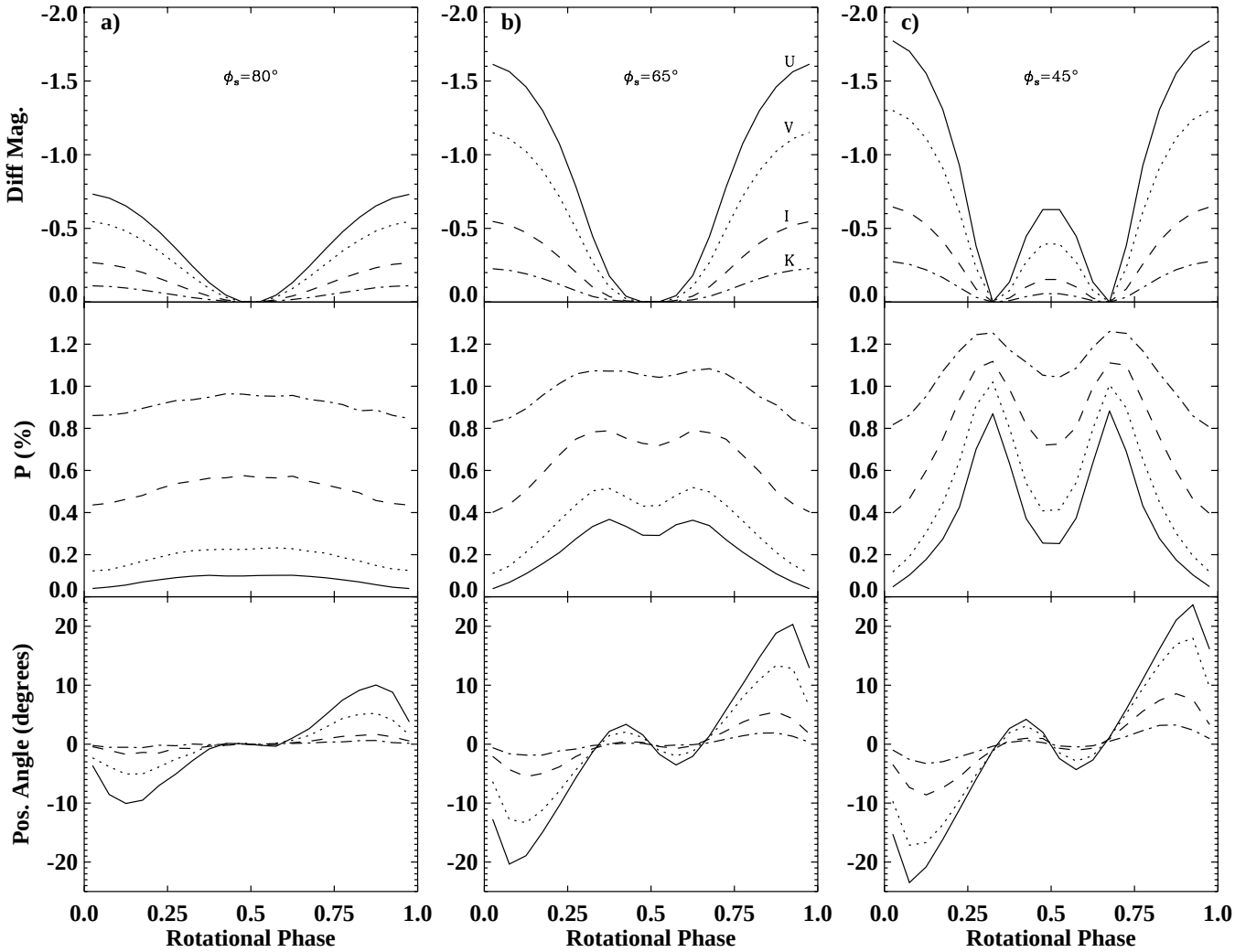

FIG. 1.—Variations in the photometry, percent polarization, and polarization position angle shown over one rotation period for three different choices of spot latitude: (*a*) $\phi_s = 80°$, (*b*) $\phi_s = 65°$, and (*c*) $\phi_s = 45°$. All other model parameters are fixed: $\theta_s = 20°$, $R_{\rm in} = 3R_*$, and $i = 63°$. In each panel, the line style indicates the four different passbands as follows: *U* (*solid line*), *V* (*dotted line*), *I* (*dashed line*), and *K* (*dot-dashed line*). Note the progression in light curve morphology, from sinusoidal to nearly flat-bottomed (see Figs. 2*a* and 3*c* for better examples of this) to double-peaked, as the spot latitude is varied. Note also the lack of variability in the percent polarization for the system with the high-latitude spots.

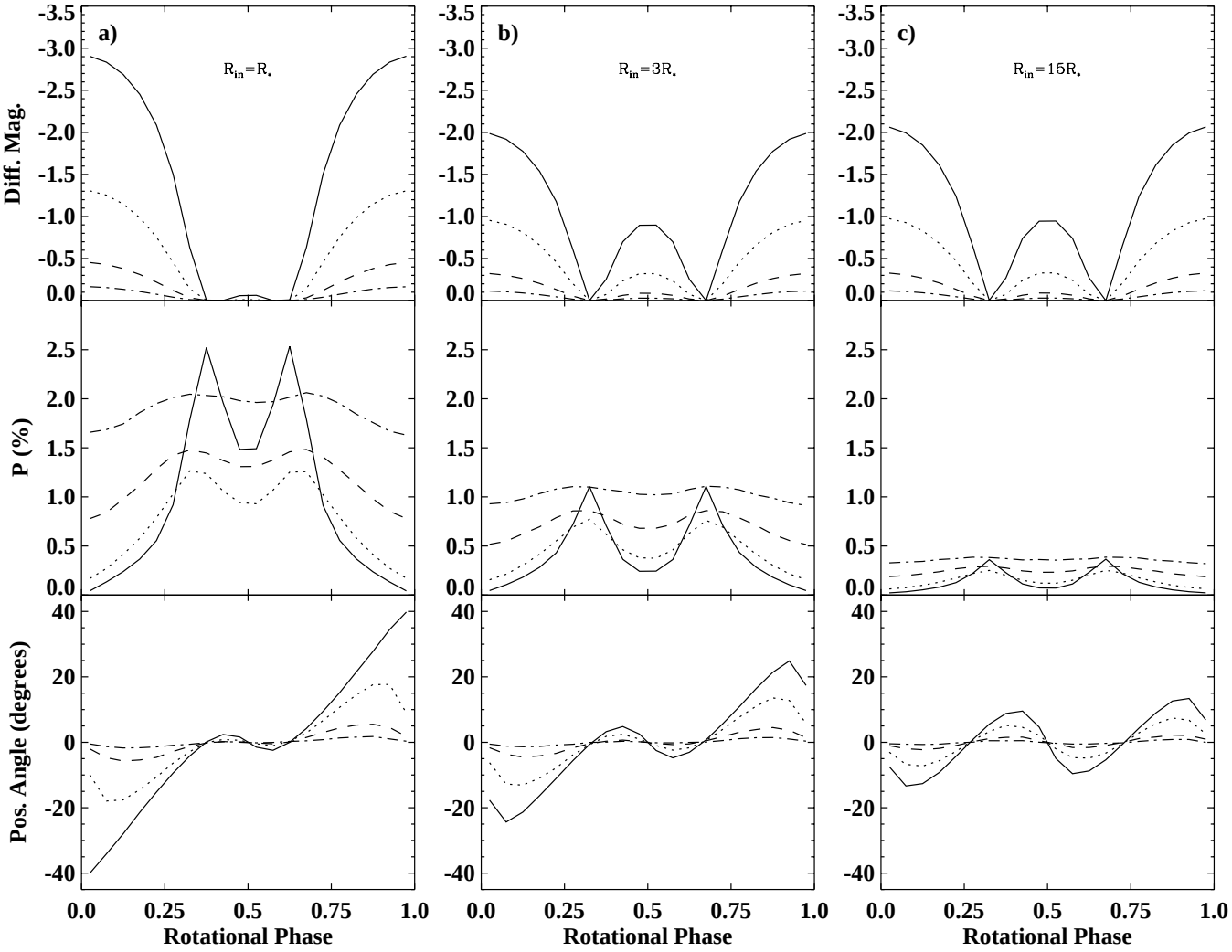

FIG. 2.—Variations in the photometry, percent polarization, and polarization position angle shown over one rotation period for three different choices of inner disk truncation radius: (*a*) $R_{in} = R_*$, (*b*) $R_{in} = 3R_*$, and (*c*) $R_{in} = 15R_*$. All other model parameters are fixed: $\theta_s = 11°.5$, $\phi_s = 45°$, and $i = 63°$. Line styles are as in Fig. 1. Note the transition from flat-bottomed to double-peaked light curve morphology as the inner disk recedes from the stellar surface. At $3R_*$, the spot on the lower hemisphere is fully revealed; the only change in increasing the disk truncation radius further is to decrease the amount of polarized radiation. Note that the small hump seen in the *U* light curve in (*a*) at phase 0.5 is a spurious feature resulting from light from the spot on the lower hemisphere leaking through the optically thin outer disk regions (see text).

photometric variability are weakly dependent on spot size; spot temperature is a far more deterministic parameter of photometric variability. Thus, the magnitude of photometric variability is not by itself a useful diagnostic for constraining spot size. However, there are cases, high-latitude spots in particular, where θ_s determines whether the spot will be completely occulted by the star as it rotates to the back side (when $\phi_s + \theta_s < i$). Flat-bottomed light curves are produced in such cases (Figs. 1*b*, 2*a*, 3*c*), in contrast to the sinusoidal light curve morphologies produced otherwise. For the range of spot sizes considered here, low-latitude spots almost invariably produce flat-bottomed light curves, except in the rare case of nearly pole-on viewing. Thus, where amplitudes of photometric variations alone do not uniquely constrain spot latitude or size, flat-bottomed light curve morphologies do suggest low-latitude spots. This is especially true if spots are believed to have large areal coverages (via, e.g., analytic modeling; see § 5), since larger spots must be situated at lower latitudes in order to be fully occulted on the back side of the star (although existing analytic modeling studies of spots on T Tauri stars have shown that hot spots tend to be small).

Despite the photometric variability produced by spots at all latitudes, we find that high-latitude spots show little ($\sim$0.1%) polarimetric variability during the rotation period (Fig. 1*a*). This is in contrast to the larger variability ($\sim$1%) seen with low-latitude spots (Fig. 1*c*). This is because the light from high-latitude spots cannot illuminate the disk at small radii where most of the polarized light originates—at small radii the disk is denser and the spot flux is larger, yielding more scattered (and hence more polarized) light. This result is contrary to the notion that hot spots necessarily give rise to rotationally modulated polarimetric variability (e.g., Gullbring & Gahm 1996). Thus, in the context of the model studied here, a lack of periodic polarimetric variability in the presence of periodic photometric variability implies high-latitude spots. As a caveat, however, we find that the presence of a large inner disk hole will suppress polarimetric variability even if the spots are at relatively low latitudes. Diagnostics of inner-disk material, such as $H-K$

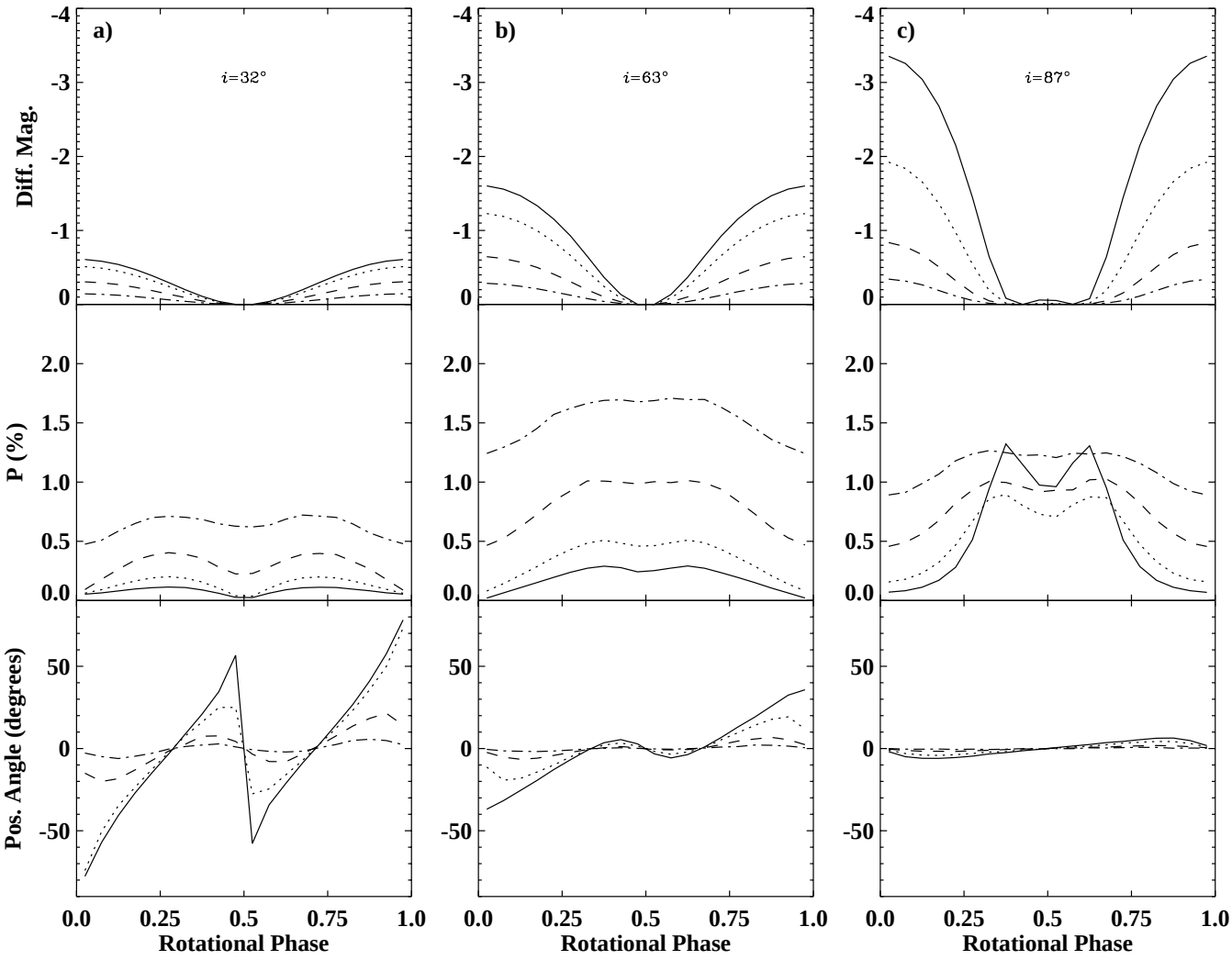

FIG. 3.—Variations in the photometry, percent polarization, and polarization position angle shown over one rotation period for three different choices of inclination angle: (*a*) $i = 32°$, (*b*) $i = 63°$, and (*c*) $i = 87°$. All other model parameters are fixed: $\theta_s = 20°$, $\phi_s = 65°$, and $R_{in} = R_*$. Line styles are as in Fig. 1. Note the progression in the amplitude of the polarization position angle variations as the system inclination is varied from pole-on to edge-on viewing. Note again the spurious feature in the *U* light curve in (*c*).

excess, can thus aid in constraining spot latitude via the polarimetric diagnostics suggested here.

An example may further elucidate the above discussion. Consider a system with observed periodic photometric variability consistent with hot spots that shows infrared signatures of inner disk material (e.g., $H-K$ excess) but that shows no periodic polarimetric variability. According to our modeling, such a system must possess spots at high latitude. For consistency, the morphology of the photometric light curve should be sinusoidal for typical spot sizes. A nonsinusoidal (i.e., flat-bottomed) morphology in this case would imply a very small spot or a very high system inclination (although flared disks will tend to bias observations against systems with high inclinations, as discussed below).

3.1.2. *Disk Truncation Radius*

Varying the disk truncation radius has a somewhat curious effect on the morphology of the photometric light curves. In particular, as the inner truncation radius is increased, certain spot latitude/system inclination geometries allow the spot on the lower hemisphere to be viewed momentarily through the inner disk hole as the star rotates. Double-peaked light curves result in such cases (Figs. 1*c*, 2*b*, and 2*c*). When these double-peaked photometric morphologies occur, we also see double-peaked variability in both the percent polarization and in the polarization position angle. Systems displaying such double-peaked light curve morphologies, especially in systems for which inner disk truncation radii are known (via, e.g., SED modeling), are narrowly constrained in the spot latitude/inclination angle parameter subspace; this double-peaked effect is not seen for spots at very high latitudes or for systems seen at very high or very low inclination angles. Thus, although observations of double-peaked light curve morphologies in systems with known inner disk holes are a potentially powerful means for constraining spot latitude and system inclination, we do not expect that such systems will occur with great frequency. This phenomenon is described more fully in the following section.

Changes in the inner disk truncation radius also have observable effects on the emergent polarization, with the percent polarization decreasing with increasing truncation radius. This is because most scattered light originates close

to the star. Removing this scattering material by increasing the truncation radius leads to a decrease in the overall level of polarization. Despite the correlation of disk truncation radius and percent polarization in our idealized treatment, we caution that percent polarization is highly degenerate in other model parameters and that the actual percent polarization scale is dependent on the poorly known scattering properties associated with the disk material.

Although our modeling indicates that photopolarimetry cannot replace the power of modeling spectral energy distributions (SEDs) as a diagnostic of disk truncation radius, our results nonetheless provide a testable prediction of magnetospheric accretion theory in systems with known inner disk holes. The observation of double-peaked light curves would offer support for the two-spot accretion geometry suggested by theory. In combination with measured SEDs, such observations can be used to constrain other system parameters, such as system inclination (see below).

3.1.3. *System Inclination*

As already stated, the system inclination is a contributing factor in the magnitude and in the morphology of the photometric variations. In particular, at higher inclinations the variability becomes greater, because a larger fraction of the visible spot disappears behind the back side of the star. The most highly inclined systems are very likely to result in flat-bottomed light curves.

Perhaps more significantly, the inclination (for favorable spot latitudes and disk truncation radii) determines whether the spot on the lower hemisphere may be seen (double-peaked light curves). Because the lower hemisphere spot can be seen for a narrow range of inclination angles (for a given spot latitude), the observation of double-peaked photometric light curves provides a constraint on the system inclination, especially if the inner disk truncation radius is known. The minimum inclination at which double-peaked light curves occur is simply that at which the second spot first becomes visible on the limb of the star, while the maximum inclination is that at which the inner edge of the disk obscures the second spot from view, given analytically by

$$i_{\max} = \cos^{-1}\left\{\frac{\sin(\phi_s - \theta_s)}{[1 + (R_{in}/R_*)^2 - 2(R_{in}/R_*)\cos(\phi_s - \theta_s)]^{1/2}}\right\}. \quad (5)$$

This result suggests that double-peaked light curve morphologies will occur only very rarely, not only because the range of inclinations that produces such morphologies is small but also because, even in those systems possessing the requisite inner disk holes, the spots must be positioned at latitudes that are lower than that expected by theory. As an example, consider a system with an inner disk radius of $R_{in} = 3R_*$, with spots at (relatively low) latitudes $\phi_s = \pm 65°$ and angular radii $\theta_s = 6.°6$. Such a system produces double-peaked light curves for inclinations in the range $60° < i < 70°$. Double-peaked light curves will be seen, therefore, in only $\sim 15\%$ of systems with this particular geometry, considering random inclination effects alone.

In general the percent polarization increases with inclination. Polarization probes the asymmetry of a system: pole-on disks are rotationally symmetric and produce no polarization, while edge-on disks present a highly asymmetric scattering surface to the observer and produce the largest polarization levels (e.g., Brown, MacLean, & Emslie 1978). As with disk truncation radius, we caution against mapping a particular percent polarization level to a particular system inclination.

In contrast to the percent polarization, changes in the polarimetric position angle are most pronounced in systems seen at low inclination (Fig. 3). Scattered light is polarized perpendicular to the plane of scattering (plane containing the incident and scattered rays). When the disk is illuminated by a bright spot, the polarization position angle is dominated by light scattered from this spot-illuminated area. As the star rotates, this area moves around the disk and the orientation of its associated scattering plane changes relative to the observer. At low inclinations, the orientation of the scattering plane relative to the observer undergoes large variations. For more inclined disks, an observer sees less variation in the orientation of the scattering planes as the spot-illuminated area moves around the disk. Therefore the largest position angle variability occurs for the pole-on systems where the scattering planes change the most during a rotation period. Position angle variability can show amplitudes of $\sim 90°$ for the most pole-on viewing angles. Indeed, periodic high-amplitude position angle variability is expected in the absence of any photometric variability in the most extreme case of directly pole-on inclination.

3.1.4. *Wavelength*

In general, the photometric behavior at the different wavelengths we studied mimic one another. The largest effect in changing the wavelength is the increased contrast between the brightness of the spot and star at shorter wavelengths, since for the chosen star and spot temperatures, we are on the Wien side of the blackbody distribution. This results in the largest photometric variability occurring at shorter wavelengths.

The blackbody contrast effect that is so prominent in the photometric variability is mitigated in the polarimetric variability by the strong wavelength dependence of the dust scattered polarization and albedo (Table 1). Although the albedo decreases toward longer wavelengths (resulting in less scattering), the increase in dust scattered polarization, p, is the dominating factor so that the polarization increases as we go into the near IR (e.g., Whitney & Hartmann 1992). Note, however, that the polarization does decrease in the near IR when we consider a flared disk geometry (see below). The blackbody contrast also results in a rotation of the polarization position angle with wavelength at a given instant. This arises because the position angle probes the axisymmetry of a system: an axisymmetric system would show no variations in position angle (or polarization) with rotational phase, and position angle variability increases as the system geometry or illumination departs from being axisymmetric. For example, at phase 1.0 in Figure 3*a*, the polarization position angle in U is near 90°, while in I it is 20°. This arises because the spot/star luminosity ratio, and hence the departure from axisymmetry, is much larger at U than at I. See § 4 for a discussion of this in relation to observations.

3.2. *Flared Disks*

Given the size of the parameter space that we chose to explore, we ran our simulations using a flat disk for expe-

diency in the Monte Carlo radiation transfer. However, disks around classical T Tauri stars are expected to have a scale height that increases with distance from the central star (e.g., Kenyon & Hartmann 1987). We therefore investigated the effect of a flared disk geometry on the photopolarimetric light curves of some of the models. The photopolarimetric variability is generally qualitatively similar to the flat disk models (Fig. 4).

There are three major differences arising from the dense flared disk. The first is that the denser disk allows for more scattered radiation and hence a higher overall percent polarization, especially at high inclinations, although the morphology of the polarimetric variations are similar to that observed for the flat disk (Fig. 5*a*). As a consequence, the flared disk allows for considerably larger polarimetric variability than the flat disk, especially at high inclinations. As an example of this, Figure 5*b* compares the polarization percent variability as a function of inclination angle, arising from the flat and flared disk models used in Figures 1 and 4. The flat disk model can produce variability in percent polarization of at most 0.3%, while the flared disk model can produce variability of 1%–5% at inclinations greater than 70°. Second, for edge-on viewing the flux is greatly reduced, since the star is viewed through the outer flared regions. This effect is displayed in Figure 5*c*, which shows the flux as a function of viewing angle for our flared disk geometry. Although the variability of the *differential* magnitude may be substantial, it is unlikely, given the large circumstellar extinctions, that the star would be detected at visible wavelengths. Indeed it is unlikely that such systems would be classified as classical T-Tauri stars (Whitney & Hartmann 1992, 1993). Finally, unlike the monotonic increase of the percent polarization with wavelength in the flat disk geometry (Figs. 1–3), the percent polarization decreases at near-IR wavelengths with the flared disk geometry (Fig. 4). This is because in our flared disk simulation the disk optical depth decreases into the IR. The combination of a lower albedo and optical depth results in less scattering and offsets the increase in dust scattered polarization with wavelength (Table 1). For high inclinations, however, when the star is occulted by the disk and the light we see is predominantly highly polarized scattered light, the polarization does increase in the IR (see also Whitney & Hartmann 1992, 1993).

3.3. *Ringlike Spots*

Recent detailed calculations of magnetospheric accretion in classical T Tauri stars has involved modeling spots as "rings" or "annuli" (Mahdavi & Kenyon 1998). Although we do not attempt to argue in this study for one spot

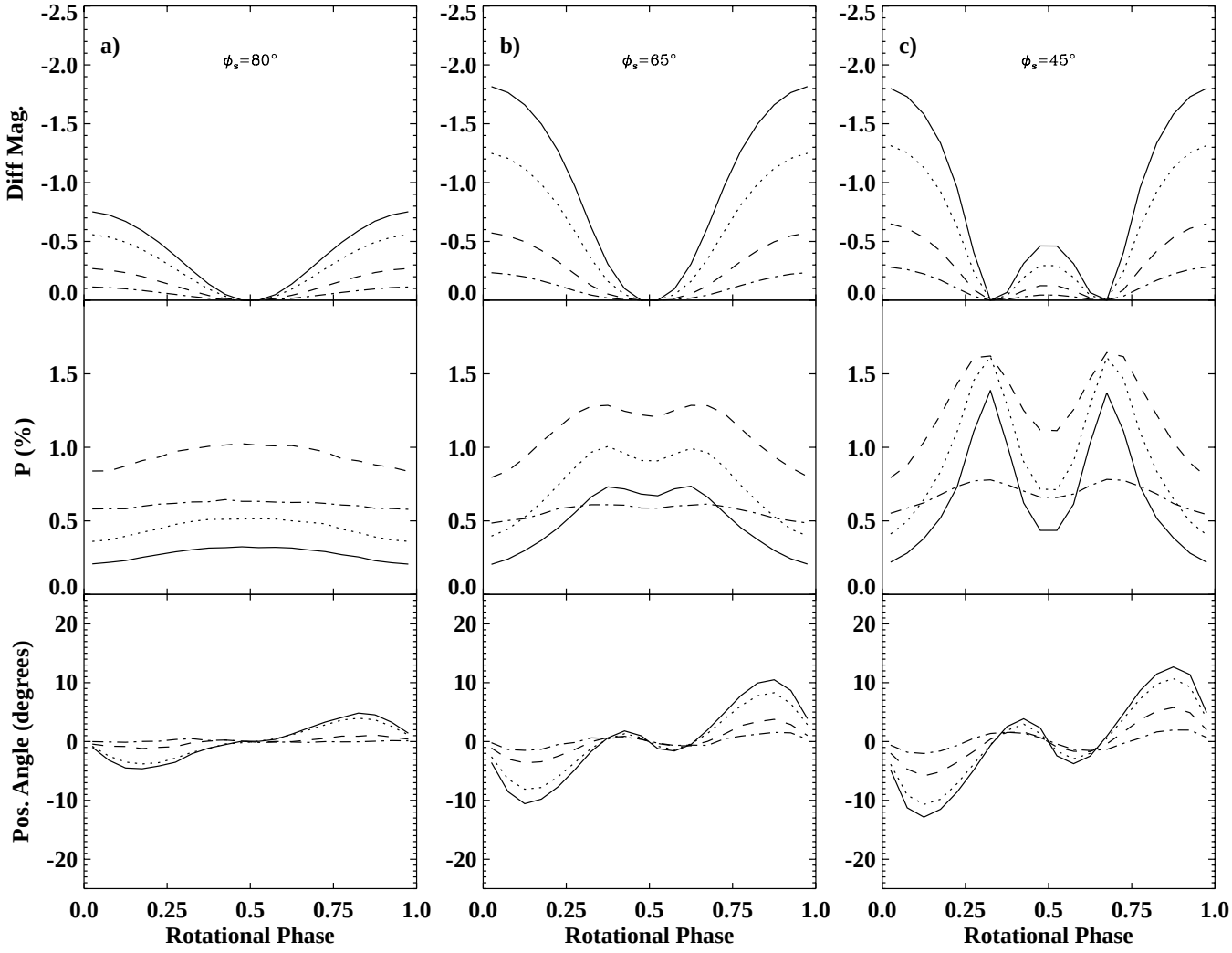

FIG. 4.—Same as Fig. 1, except with flared disk geometry. Note the change in polarimetric behavior in *K*.

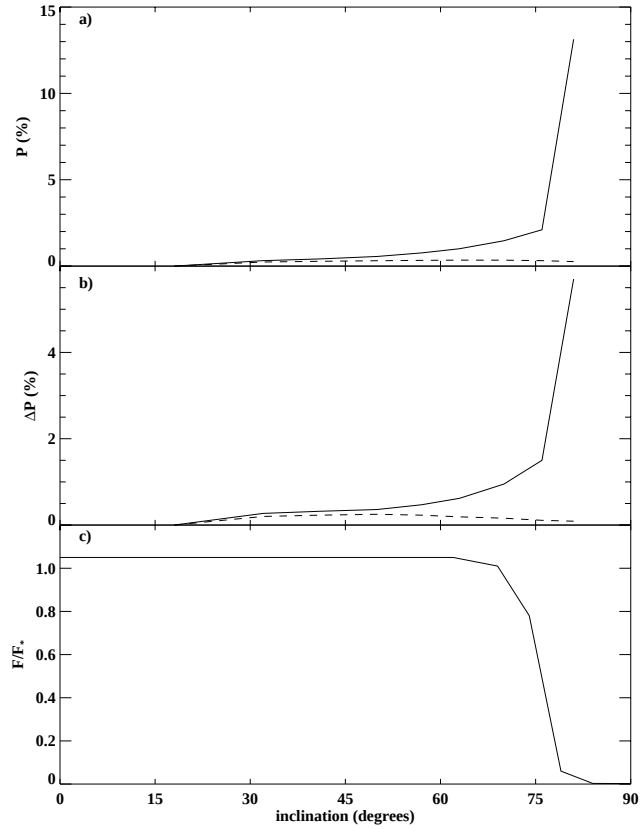

FIG. 5.—Salient differences between flared and flat disk geometries: (*a*) Maximum polarization (at *V*) as a function of inclination angle for a model with a flared disk (*solid line*) and the same model with a flat disk (*dashed line*). Model parameters are as in Fig. 1*b*. (*b*) Same as (*a*) except polarization variability is shown. (*c*) Fraction of emergent light relative to the intrinsic stellar output is shown as a function of system inclination for the flared disk geometry. For inclinations $i > 70°$, the outer regions of the flared disk intercept an increasingly larger fraction of stellar photons. The emergent fraction exceeds unity for $i < 70°$ because the disk scatters additional light to the observer.

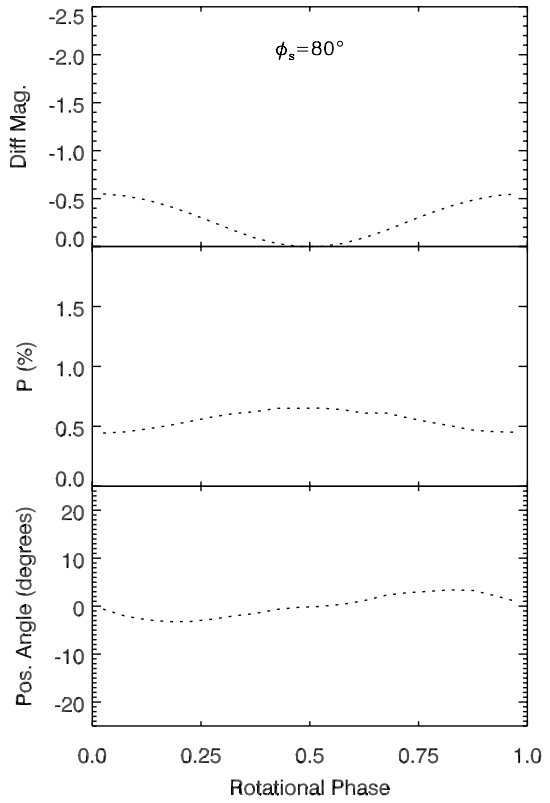

FIG. 6.—Same as Fig. 4*a* (*V* band only) except with ringlike spots. The rings have an outer radius of 23° and an inner radius of 10°, giving them the same areal coverage as the spots in Fig. 4*a*.

geometry over another on a theoretical basis, we do comment on the effect of a ringlike spot geometry on the photopolarimetric observables we have modeled.

We generated a single model (with a flared disk), employing typical system parameters at one wavelength (Fig. 6), to see if we could detect any significant differences in the resulting photopolarimetric behavior that might allow one to distinguish between accretion rings and spots on the basis of photopolarimetry. We find no such differences. As with filled-in spots, the morphology of the photometric variation is sinusoidal, its amplitude consistent with the areal coverage of the ring (see Fig. 4*a*). Our modeling thus suggests that photopolarimetry may not be useful for distinguishing fine details of accretion spot geometry.

4. COMPARISON TO OBSERVATIONS

Hot spots have been implicated in the observation of periodic photometric variability in scores of T Tauri systems (e.g., Bouvier et al. 1993). Hot spots are also suspected to be the cause of the more erratic variability seen in the large amplitude irregular variables (e.g., Eaton, Herbst, & Hillenbrand 1995). This may arise because accretion onto hot spots is likely to be dynamically active. Thus, morphologies of hot spot light curves are likely to behave more stochastically than the strictly periodic behavior of our model systems. Nonetheless, stable periodic variability arising from hot spots has been seen (Choi & Herbst 1996; Herbst et al. 1994; Bouvier et al. 1993). Bouvier et al. (1993) find that hot spots are present in the majority of the classical T Tauri stars in their sample, indicating that hot spots do sometimes exist stably for timescales long compared to one stellar rotation period. Bouvier et al. (1993) further find that hot spots typically cover only a few percent of the stellar surface, consistent with our use of relatively small spots in our models.

Observational studies have shown that, almost without exception, the periodic photometric variations of T Tauri stars have a sinusoidal morphology. The morphology of our photometric light curves are generally sinusoidal except when the spots are occulted (giving flat-bottomed light curves) or at low latitude and the second spot is seen (giving double peaked light curves). Bouvier & Bertout (1989) model one star they observed (DF Tau) with a flat bottomed light curve. But such light curve morphologies have been seen only rarely. The observational absence of flat-bottomed morphologies indicates that spots are at least partially visible throughout the stellar rotation period. On the basis of our modeling, this suggests that high-latitude spots prevail among those systems that have been studied, since low-latitude spots will be occulted by the star unless the system is viewed almost pole-on. Our models further indicate that these systems are predominantly observed at low inclination, since even at high latitude a spot can be

occulted if viewed at high inclination. We do note that flat-*topped* light curves due to cool spots have been observed more frequently (e.g., Bouvier & Bertout 1989), suggesting that cool spots do occur at low latitudes or that some systems with cool spots are observed at high inclination. Indeed, it is not surprising within the context of the magnetospheric accretion paradigm that only cool spots are observed in stars seen at high inclination; hot spots will only be observed on stars with circumstellar disks, which will tend to bias observations against highly inclined systems.

The amplitudes of photometric variability seen in our models, $\Delta I \lesssim 1$ mag (see Figs. 1–3), are generally consistent with those observed (see Mahdavi & Kenyon 1998 for histograms of photometric variability in Taurus-Auriga and Orion). It should be noted that the samples used in studies of periodic photometric variability (e.g., Bouvier et al. 1993; Herbst et al. 1994; Choi & Herbst 1996) almost certainly contain a mix of classical and weak-lined T Tauri stars. It is thus unclear the extent to which observations of periodic photometric variability are dominated by cool spots, bearing no connection to the magnetic accretion model studied here. Nonetheless, our models demonstrate that hot spots can account for the observed range of photometric variability among periodic variables. Large-amplitude irregular variables have been observed with somewhat larger amplitudes of variability, sometimes exceeding 2 mag at I (Choi & Herbst 1996). This is larger than that produced in any of our models, indicating that such large amplitude variations are likely due to larger spot/star temperature ratios than simulated in our models. (Choi & Herbst 1996 attribute some of these large amplitude irregular variations to obscuration by circumstellar material on the basis of light curve morphology.)

Double-peaked light curves only occur when both spots can be seen during the rotation period, arising from a favorable combination of spot latitude and inner disk hole size. Systems with known inner holes (as inferred from modeling of SEDs) should be monitored for this effect. To date, there have been no reports of double-peaked light curves attributable to hot spots. But if this effect is present and strong (i.e., the second spot is as bright as the primary), it could mistakenly result in a period determination that is half of the true rotation period, as has occurred in JW 191 (Choi & Herbst 1996). Although double-peaked light curves do not guarantee that the second spot is located on the lower hemisphere, such morphologies are nonetheless predicted by the magnetic accretion model, and the observation of such, especially when the two spots are separated in phase by close to 180°, merits special attention.

Polarization studies of T Tauri stars have been more carefully directed than photometric variability studies at classical T Tauri stars. Even so, we caution that classical T Tauri status does not guarantee the presence of hot spots (e.g., Bouvier et al. 1993). Ideally, a measure of spot temperature (see § 5) would accompany future polarimetric variability studies. The polarization levels seen in our models are consistent with those observed. Menard & Bastien (1992) present a distribution of observed linear polarization levels for 122 stars and find a most common value of $\sim 1\%$ with a long tail extending to polarizations as high as $\sim 15\%$. Figures 1–3 show representative polarizations of $\sim 1\%$–2% but none as high as the largest observed. Such a large polarization can only be reproduced in our models when we employ a flared disk at a relatively high inclination (see Fig. 5*a*). At such high inclinations, reddening due to circumstellar dust in the flared disk becomes non-negligible (Fig. 5*c*) so that our models predict that systems exhibiting polarizations larger than $\sim 3\%$ should also be highly reddened (e.g., HL Tau; Menard & Bastien 1992).

Polarimetric variability has been observed in many systems, typically at levels of $\lesssim 0.5\%$ and only occasionally at levels of up to a few percent (Gullbring & Gahm 1996). The results of our models are consistent with this (Figs. 1–4), but in our models variations in polarization $\gtrsim 1\%$ require flared disks at high inclination (Fig. 5*b*). Unfortunately, little synoptic photopolarimetric variability work has been carried out, with most of the existing observations (e.g., Schulte-Ladbeck 1983; Drissen et al. 1989; Menard & Bastien 1992; Gullbring & Gahm 1996) either having sparse time-sampling or being relatively well-sampled but spanning only a few days. Periodicities have been suggested for only a few systems (see, e.g., Menard & Bastien 1992; Drissen et al. 1989) but not yet solidly confirmed for any. Menard & Bastien propose several mechanisms for the polarimetric variability they observe, including star spots and inhomogeneities in the circumstellar environment, and exclude spots as the likely source of the polarimetric variability because of this apparent absence of periodic modulations and to the lack of periodic photometric variability on polarimetrically variable stars. It should be emphasized that very little of the existing photopolarimetric monitoring work has been well suited for finding the 1–10 day periods that typify T Tauri stars (Choi & Herbst 1996); the interpretation that polarimetric variability is never periodic is far from secure. In order for disk inhomogeneities to produce nonperiodic variability, the disk density structure would have to change on short timescales since any inhomogeneous disk structure which is stable over a few orbital periods would produce periodic variability. Alternatively, if accretion streams are present (as in the magnetospheric accretion model), these present a natural system asymmetry and source for scattered polarization. If the accretion flow in these streams is time variable, they may provide the inhomogeneities proposed by Menard & Bastien. This will be investigated in a future paper. On the basis of our models, a *lack* of polarimetric variability could simply be the result of high-latitude spots. Indeed, many of the systems observed by Menard & Bastien (1992) show little to no polarimetric variability but show substantial (i.e., $\Delta\theta > 45°$) position angle variations (see their Table 4), as seen in our models with high-latitude spots observed at low system inclination (e.g., Fig. 3*a*).

A common feature among much of the existing photopolarimetric monitoring studies of T Tauri stars is the stochasticity of the polarimetric variability. Our model systems display only strictly periodic behavior, because we did not include any stochastic component to our simulations. To explore the extent to which the magnetic accretion model can help explain systems displaying stochastic polarimetric behavior, we have generated a model (the same model as in Fig. 3*b*) in which we allow the spot size to vary randomly over three stellar rotations so as to simulate, if only crudely, the effect of variable accretion. The resulting polarimetric variability is shown in Figure 7*a*. This type of variability, if observed, would likely be interpreted as random variations. Yet a clear correlation is present between the polarimetric

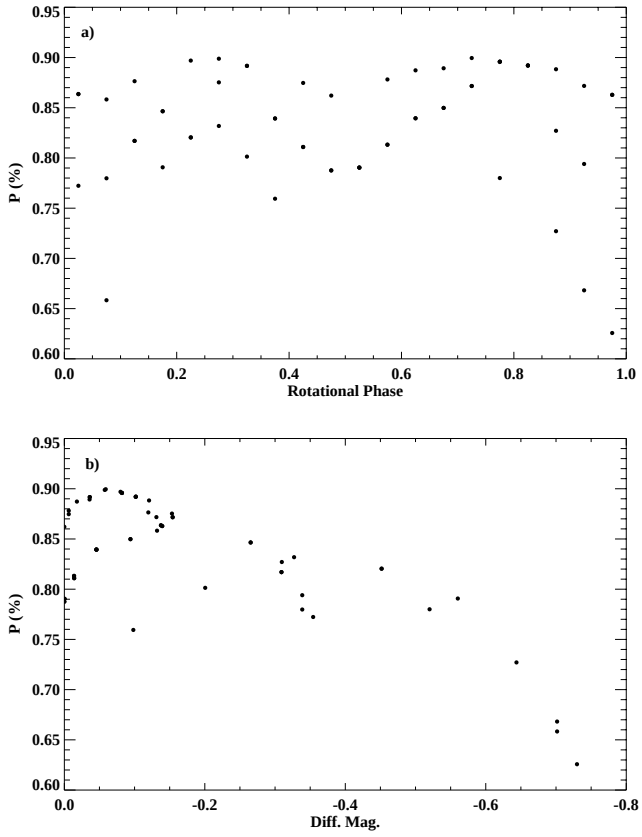

FIG. 7.—Time-variable photopolarimetry arising from a model (parameters same as in Fig. 3*b*, *I* band) in which variable (random) accretion is simulated over three stellar rotations. Panel (*a*) gives the percent polarization. Although individually stochastic, the photometric and polarimetric variability are correlated in the sense of minimum polarization at maximum brightness (*b*).

and photometric variability (Fig. 7*b*), in the sense of minimum polarization at maximum brightness. This type of correlation has been observed in several systems (see Gullbring & Gahm 1996, but see Fig. 2 of Drissen et al. 1989 for a plot of RY Lup similar to our Fig. 7*b*). We do not find any reported clear instances of systems in which polarimetric variability in the absence of correlated photometric variability is observed. Such cases would not be explained by our models and would require mechanisms other than those investigated in our models, such as time-variable inhomogeneities in the circumstellar environment (as suggested above, the accretion streams inherent to the magnetic accretion model might provide a natural explanation for these systems).

Our models predict that the percent polarization increases with wavelength (although our flared disk simulations do show a polarization turnover at *K*). This at first appears contrary to observations, which typically show a wavelength dependence of the polarization that peaks around the *V* band (e.g., Gullbring & Gahm 1996). However, these observations have not been corrected for the effects of interstellar polarization. The wavelength dependence of interstellar polarization follows a "Serkowski Law" (Serkowski, Mathewson, & Ford 1975), which peaks at visual wavelengths. Since previous studies have focused on differential polarimetry, the intrinsic polarization spectrum of these stars is undetermined. A careful analysis of spectropolarimetric data with accurate interstellar removal is therefore required before we can directly compare our wavelength dependent polarization model predictions with observations. Gullbring & Gahm (1996) have noted that the measured position angle for V1121 Oph at a given time is not independent of wavelength, with a maximum rotation from *U* to *I* of 43°. They attribute this to a wavelength-dependent interstellar polarization component. But this behavior is consistent with many of our model systems in which differences of $\sim 45°$ in position angle between *U* and *I* are seen at certain phases. To be entirely consistent with our models, observed differences in position angles at different wavelengths should vary as a function of phase (e.g., Fig. 3*a*).

In our models, we have not included cool spots, which are often the primary source of periodic photometric variability in classical T Tauri stars (Bouvier et al. 1993). As such, our model predictions of photometric variability only apply to cases where hot spots are present and dominant. Our model predictions of polarimetric variability, however, are not likely to be severely affected by our omission of cool spots. Hot spots, which in our models have luminosities comparable to stellar, produce polarimetric variability because of their large illuminating asymmetry. Cool spots, which are typically only a few hundred degrees cooler than photospheric (Bouvier et al. 1993), do not present such a large asymmetry and will consequently result in smaller polarization levels and polarimetric variability.

5. ANALYTIC INVERSION

Analytic inversion techniques are commonly employed to determine spot properties such as temperature and areal coverage. In its most simple incarnation, this technique basically consists of a two-component blackbody fitted to the observed *amplitudes* of periodic photometric variability at multiple wavelengths. Usually, the stellar temperature is known (through the stellar spectral type), minimizing the number of free parameters to two: spot temperature and size. Although this type of analytic modeling has been applied by various authors throughout the literature, no analyses of the reliability of such modeling have been reported (but see the statistical analysis of Levenberg-Marquardt techniques by Kővári & Bartus 1997). Typically, spot parameters reported on the basis of analytic inversion techniques are reported with uncertainties of ~ 100 K in temperature and a few percent in areal coverage.

We have applied an analytic inversion method to our simulated light curves in order to ascertain the reliability of such modeling in accurately recovering spot properties. For specificity, we adopt a model similar to that employed by Bouvier et al. (1993) and Vrba, Herbst, & Booth (1988) in which the wavelength-dependent amplitude of photometric variation, $\Delta m(\lambda)$, is parametrized in terms of the spot-to-star flux ratio, $Q(\lambda)$, and the projected minimum and maximum spot areal coverage, f_1 and f_2:

$$\Delta m(\lambda) = -2.5 \log \left\{ \frac{1 - [1 - Q(\lambda)] f_2}{1 - [1 - Q(\lambda)] f_1} \right\} . \quad (6)$$

Unlike these authors, we do not consider the effects of limb darkening or a radiation distribution more sophisticated than a simple blackbody, because our current Monte Carlo simulation does not employ model atmospheres.

We find that this simple model is able to accurately reproduce the known spot temperature and size in each of our Monte Carlo simulations. This is perhaps not surprising, considering that the simulations consist—as does the analytic model—of two simple blackbody components and that our simulated light curves are noiseless. But to what extent can spot parameters be constrained when real (i.e., noisy) data are modeled? In order to quantify this, we investigated the dependence of the size of the solution space as a function of noise in the input data. We generated 1000 $\{\Delta U, \Delta V, \Delta I, \Delta K\}$ sets for each of our models by adding normally distributed noise with standard deviations of 0.01, 0.03, and 0.05 mag to the known Δm. We then computed best-fit values of T_s, f_1, and f_2 via equation (6) above for each $\{\Delta U, \Delta V, \Delta I, \Delta K\}$ set using a χ-square minimization technique; we then take the region of the parameter space containing 95% of these best-fit values as the region of 95% confidence (Press et al. 1992).

We find that the spot temperature is significantly more sensitive to noise in the photometric amplitudes than previous use of this type of analysis suggest. Even for modest uncertainties in the data ($\sigma_{\Delta m} = 0.01$), spot temperatures between 7500 and 15,000 K yield strong goodness-of-fit for the particular case shown in Figure 8*c*. In contrast, spot sizes only vary between 3% and 12% in this case, small by most standards. This suggests that error estimates of spot temperatures commonly quoted in the literature where this type of analytic inversion is used (e.g., Bouvier et al. 1993) may be underestimated. We note that this basic conclusion is similar to the results of Kővári & Bartus (1997), who find that photometric uncertainties of order 1% are sufficient to make their spot parameter determination become unstable. We further find that the largest density of solutions for photometric amplitude uncertainties of $\gtrsim 3\%$ occurs at spot temperatures that are cooler—and spot sizes that are larger—than the true values. This feature of the solution space may serve to partially compensate for the tendency to underestimate spot sizes due to projection effects (Bouvier et al. 1993).

Despite this difficulty in accurately determining spot temperatures given even small formal uncertainties in photometric amplitudes, we find that it is relatively straightforward to distinguish hot spots from cool ones. In fact, we find that it is nearly impossible to force the analytic inversion studied here to incorrectly label a hot spot as a cool one, assuming "reasonable" uncertainties in the photometric data (pathological solutions—e.g., a cool "spot" covering 95% of the surface—excluded). For the case considered in Figure 8, cool spots are not inferred with any frequency until noise of order 0.20 mag is added to the photometric amplitudes.

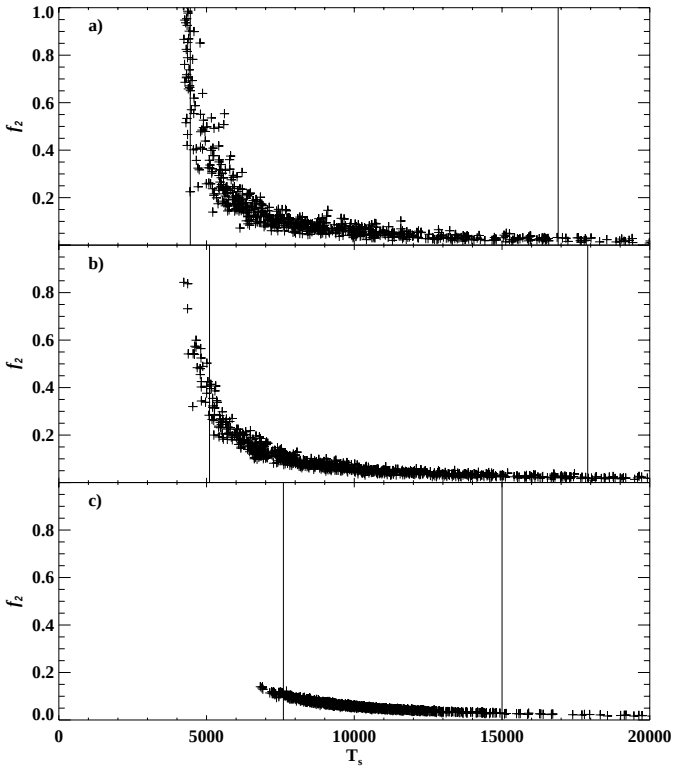

FIG. 8.—Parameter subspace T_s vs. f_2 shown for analytic fits to the photometric amplitudes of the model with $\phi_s = 65°$, $\theta_s = 20°$, $R_{in} = 3R_*$, and $i = 32°$. The true spot parameters are $T_s = 10{,}000$ K, $f_2 = 0.06$. Shown are the best-fit spot parameters to 1000 realizations of the photometric amplitudes with 0.05 (*a*), 0.03 (*b*), and 0.01 (*c*) mag noise. The vertical lines contain 95% of the points about the true temperature. Note the asymptotic behavior at low values of the spot temperature as the stellar temperature ($T_* = 4{,}000$ K) is approached, and the high density of points at spot temperatures/sizes that are cooler/larger than the actual values (see text).

6. SUMMARY AND CONCLUSIONS

We have modeled the photopolarimetric variations arising from a classical T Tauri star/disk system possessing hot spots on the stellar surface in an attempt to identify useful observational diagnostics of system parameters of interest and to assess the ability of the magnetic accretion model to explain existing observations of photopolarimetric variability in T Tauri stars. Although we have restricted our attention in this initial study to a simple interpretation of magnetospheric accretion, the Monte Carlo technique we employ can be applied to any other model of interest (e.g., flared disks, hot "rings," cool spots, and stellar atmospheres). We will investigate the effects of the actual magnetospheric accretion flow on observed polarimetric variability in a future study.

On the basis of our modeling, we confirm that the magnetic accretion model is consistent with existing observations of photopolarimetric variability in T Tauri stars and have identified the following observational diagnostics of key system parameters. These serve as testable predictions of the magnetospheric accretion model and as a guide to future photopolarimetric monitoring studies of T Tauri stars:

1. Double-peaked light curves reveal the existence of a spot on lower hemisphere. This effect requires a favorable combination of spot latitude, system inclination, and inner disk truncation radius. In particular, if a "typical" disk truncation radius of $R_{in} = 3R_*$ is assumed, spots must be situated at low latitudes ($\phi_s \lesssim 60°$) and the system inclination is somewhat constrained ($\phi_s \lesssim i \lesssim 75°$). Given the theoretical bias against such low-latitude spots and the small region of parameter space occupied by the appropriate combination of system parameters, we do not expect that such double-peaked light curve morphologies will occur with great frequency. We note, however, that Choi & Herbst (1996) have observed "period-doubling" in JW191, presumably the result of a second spot.

2. Flat-bottomed light curves (the spot is completely occulted by the star) imply a low spot latitude. For low inclinations, a flat-bottomed morphology could imply a high-latitude spot of very small size. In these cases, analytic inversion techniques such as that employed by Bouvier et al. (1993) can provide an independent estimate of spot size. The general lack of this morphology among hundreds of systems observed suggests that low-latitude spots and high inclination rarely, if ever, occur among classical T Tauri stars.

3. Large polarization position angle variations are strongly indicative of low inclination. Figure 3 shows how amplitude of position angle variability is related to inclination. The effect is most prominent in the U band, where the spot radiates most efficiently relative to the photosphere.

4. Large percent polarization variations ($\gtrsim 1\%$) and/or high polarization values ($\gtrsim 3\%$) require a flared disk geometry. Systems exhibiting very large polarizations will likely be highly reddened by circumstellar dust in the flared disk.

5. A lack of variability in linear polarization (in the presence of photometric variability) is indicative of high-latitude spots. Figure 1 shows how a spot situated at high latitude does not produce significant polarization variability despite significant photometric variability. This is contrary to the periodic variability commonly expected in polarization variability studies. Hot spots have been mistakenly discounted in systems where no polarimetric variability has been observed (e.g., Menard & Bastien 1992; Gullbring & Gahm 1996). If high-latitude spots are common among classical T Tauri stars, we expect that such behavior will typify observations of these objects. Such systems observed at low inclination will display large position angle variations despite showing no discernible variability in linear polarization. Numerous such cases have been observed (see Menard & Bastien 1992). Hot spots have also been discounted in systems in which polarimetric variability is highly stochastic. In this case, hot spots may also be responsible if anticorrelated photometric variability is observed (in the sense of minimum polarization at maximum brightness).

We find that wavelength-dependent polarization position angles arise naturally in our models and do not require the invocation of multiple interstellar polarization components.

We find that disk truncation radius is not prescriptive of either the photometric or the polarimetric observational diagnostics considered in this study. However, cleared inner disk regions are required if the double-peaked light curve morphology discussed above is to be observed.

These results are not significantly altered when we model accretion spots as rings.

Lastly, we confirm the applicability of analytic inversion techniques for recovering spot properties such as size and temperature from observations of periodic photometric variability at multiple wavelengths. We find that observational uncertainties will tend to cause such techniques to err more strongly in determining spot temperatures than has been suggested by some reports in the literature employing this type of analysis. We also find that solutions tend to systematically underestimate spot temperatures and to overestimate spot sizes. To the extent that one is interested simply in determining whether spots are hotter or cooler than stellar photospheres, we find that a technique similar to that employed by Bouvier et al. (1993) and Vrba et al. (1988) does so reliably. This result is encouraging, considering that studies of periodic photometric variability in young stars are often concerned with simply determining whether spots are hot or cool.

We thank Scott Kenyon, Robert Mathieu, Barbara Whitney, David Cohen, and Gina Brissenden for useful discussions. This paper was improved considerably by criticisms from an anonymous referee. This work has been funded through an NSF graduate student fellowship and a grant from NASA's Long-Term Space Astrophysics Research Program (NAG 5-6039). The radiation transfer models were run on the SGI cluster at the University of Wisconsin Astronomy Department.

REFERENCES

Adams, F. C., Lada, C. J., & Shu, F. H. 1987, ApJ, 312, 788
Attridge, J. M., & Herbst, W. 1992, ApJ, 398, L61
Basri, G., & Batalha, C. 1990, ApJ, 363, 654
Basri, G., & Bertout, C. 1989, ApJ, 341, 340
Bastien, P., & Menard, F. 1988, ApJ, 326, 334
Beckwith, S. V. W., Sargent, A. I., Chini, R. S., & Güsten, R. 1990, AJ, 99, 924
Bouvier, J., & Bertout, C. 1989, A&A, 211, 99
Bouvier, J., Cabrit, S., Fernandez, M., Martin, E. L., & Matthews, J. M. 1993, A&A, 61, 737
Brown, J. C., MacLean, I. S., & Emslie, G. A. 1978, A&A, 68, 415
Choi, P. I., & Herbst, W. 1996, AJ, 111, 283
Draine, B. T. 1985, ApJS, 57, 587
Draine, B. T., & Lee, H. M. 1987, ApJ, 318, 485
———. 1984, ApJ, 285, 89
Drissen, L., Bastien, P., St. Louis, N. 1989, AJ, 97, 814
Eaton, N. L., Herbst, W., & Hillenbrand, L. A. 1995, AJ, 110, 1735
Edwards, S., Hartigan, P., Ghandour, L., & Andrulis, C. 1994, AJ, 108, 1056
Fischer, O., Henning, T., & Yorke, H. W. 1994, A&A, 284, 187
Ghosh, P., & Lamb, F. K. 1979a, ApJ, 232, 259
———. 1979b, ApJ, 234, 296
Gullbring, E., & Gahm, G. F. 1996, A&A, 308, 821
Hartmann, L., Hewett, R., & Calvet, N. 1994, ApJ, 426, 669
Herbst, W., Herbst, D. K., Grossman, E. J., & Weinstein, D. 1994, AJ, 108, 1906
Joy, A. 1945, ApJ, 102, 168
Kenyon, S. J., & Hartmann, L. 1987, ApJ, 323, 714
Kenyon, S. J., Yi, I., & Hartmann, L. 1996, ApJ, 462, 439
Kenyon, S. J., et al. 1994, AJ, 107, 2153
Königl, A. 1991, ApJ, 370, L39
Kővári, Z., & Bartus, J. 1997, A&A, 323, 801
Mahdavi, A., & Kenyon, S. J. 1998, ApJ, 497, 342
Makidon, R. B., Strom, S. E., Tingley, B., Adams, M. T., Hillenbrand, L., Hartmann, L., Calvet, N., & Jones, B. F. 1997, BAAS, 191, 5.06
Mathis, J. S., Rumpl, W., & Nordsieck, K. H. 1977, ApJ, 217, 425
Menard, F., & Bastien, P. 1992, AJ, 103, 564
Najita, J. 1995, Rev. Mexicana Astron. Astrofis., 1, 293
Ostriker, E. C., & Shu, F. H. 1995, ApJ, 447, 813
Press, W. H., Teukolsky, S. A., Vetterling, W. T., & Flannery, B. P. 1992, Numerical Recipes in FORTRAN (2d ed.; Cambridge Univ. Press)
Shulte-Ladbeck, R. 1983, A&A, 120, 203
Serkowski, K., Mathewson, D. L., & Ford, V. L. 1975, ApJ, 196, 261
Shakura, N. I., & Sunyaev, R. A. 1973, A&A, 24, 337
Shu, F. H., Najita, J., Ostriker, E. C., Wilkin, F., Ruden, S., & Lizano, S. 1994, ApJ, 429, 781
Vrba, F. J., Herbst, W., & Booth, J. F. 1988, AJ, 96, 1032
Vrba, F. J., Rydgren, A. E., Chugainov, P. F., Shakovskaya, N. I., & Zak, D. S. 1986, ApJ, 306, 199
White, R. L. 1979, ApJ, 229, 954
Whitney, B. A., & Hartmann, L. 1992, ApJ, 395, 529
———. 1993, ApJ, 402, 605
Whitney, B. A., Kenyon, S. J., & Gómez, M. 1997, ApJ, 485, 703
Wichmann, R., Bouvier, J., Allain, S., & Krautter, J. 1998, A&A, 330, 521
Wood, K., Kenyon, S. J., Whitney, B. A., & Bjorkman, J. E. 1996, 458, L79